Earth and Planetary Science Letters 388 (2014) 249–256

Contents lists available at ScienceDirect

Earth and Planetary Science Letters

www.elsevier.com/locate/epsl

The giant coastal landslides of Northern Chile: Tectonic and climate interactions on a classic convergent plate margin

Anne E. Mather [a,*], Adrian J. Hartley [b], James S. Griffiths [a]

[a] School of Geography, Earth and Environmental Sciences, Plymouth University, Plymouth, Devon PL4 8AA, UK
[b] Department of Geology and Petroleum Geology, University of Aberdeen, Aberdeen AB24 3UE, UK

ARTICLE INFO

Article history:
Received 14 October 2012
Received in revised form 8 October 2013
Accepted 9 October 2013
Available online 30 December 2013
Editor: P. Shearer

Keywords:
giant landslides
Andean forearc
tectonics
geomorphology
geohazard
Atacama

ABSTRACT

Documented for the first time are an extensive suite of late Neogene giant terrestrial coastal landslides along the classic convergent margin of western South America (18° to 24° south). These are remarkable in terms of their unusual abundance and atypical setting, such failures previously being linked with oceanic volcanic edifices or over-steepened glaciated coastlines. Located within the hyper-arid Coastal Cordillera of the Atacama Desert of Northern Chile we report the presence of more than 60 individual large-scale landslides with individual volumes up to 9 km^3 developed over a horizontal coastline distance of some 650 km. These landslides were emplaced as a combination of rock avalanches and multiple rotational failures. The majority terminated directly into the Pacific – likely generating significant tsunami hazard to the Chilean and south Peruvian coastline in a region which is today considered to be part of a notorious seismic gap. The proliferation and scale of these Late Neogene giant landslides in this actively uplifting, hyperarid terrain suggests they are the main geomorphic agent for relief reduction, probably triggered by megathrust earthquakes and potentially providing a unique palaeoseismic archive. The temporal and spatial distribution of these giant landslides corresponds with a period of surface steepening of the forearc wedge in the Central Andes and south to north differential uplift associated with factors such as aseismic ridge subduction. The resulting surface gradient increases, combined with the persistent climatic aridity of the region, have served to limit effective relief-reducing geomorphic processes in this oversteepened terrain to large-scale landsliding. The phenomena documented here geospatially link previously recognised large-scale slope failures from the off-shore environment and higher altitude areas of the Andean forearc, suggesting that large-scale landsliding is capable of transferring sediment on a regional scale to the off-shore Peru–Chile trench. This has implications for the friction of the subducting Nazca plate and associated seismicity and uplift.

1. Introduction

The lateral collapse through large-scale landsliding of mid-oceanic volcanic islands formed over mantle hot spots is well-documented (Keating and Mcguire, 2000; Masson et al., 2002). It is also believed that these failures have been responsible for mega-tsunamis affecting coastlines in Australia and the eastern seaboard of North America (Ward, 2001; Whelan and Kelletat, 2003). However, there appears to have been less investigative work on the potential landslide and commensurate tsunami hazard associated with subduction zone boundaries, despite the obvious similarity of rapid uplift creating highly over-steepened slopes. Indeed the increased seismic hazard in a subduction zone compared to mid-oceanic volcanic islands would suggest that the occurrence and magnitude of geohazards in these areas would be greater. In this study remote sensing and field investigations of the seaward scarp of the Coastal Cordillera in Northern Chile has revealed previously unreported large terrestrial landslides and features indicative of giant landslide backscars. The scale of landsliding represented by these features is comparable in size to the failures reported from Hawaii (Moore et al., 1994; Clague and Moore, 2002) and the Canary Isles (Masson et al., 2002) suggesting a significant but presently unrecognised natural hazard to development in this and other regions of comparable geological setting. We document for the first time the presence of giant terrestrial landslides (volumes of $> 10^8$ m^3 and areas of 10^0 to 10^3 km^2; Korup et al., 2007) along the coastal margin (Coastal Cordillera) of the Central Andean forearc of western South America (18° to 24° south, some 650 km). The Central Andes is often cited as the type example of a convergent continental margin wherein the forearc is an important element that directly reflects the interaction between the subducting and overriding plates. Thus within this context an understanding of the dominant terrain shaping geomorphic processes can provide insights into the nature of the regional deformation

* Corresponding author.
E-mail address: amather@plymouth.ac.uk (A.E. Mather).

0012-821X/$ – see front matter
http://dx.doi.org/10.1016/j.epsl.2013.10.019

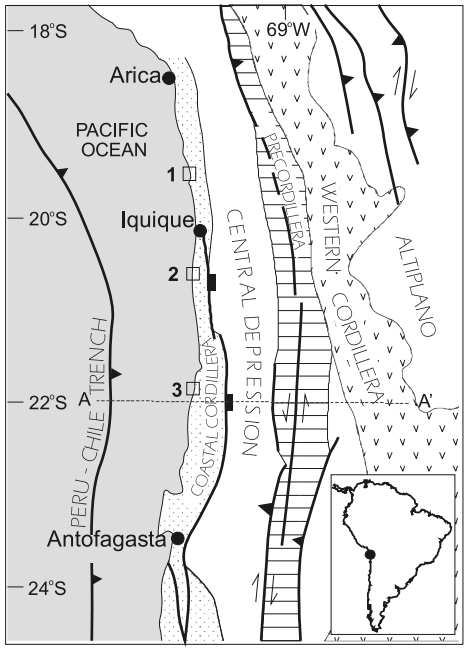

(a)

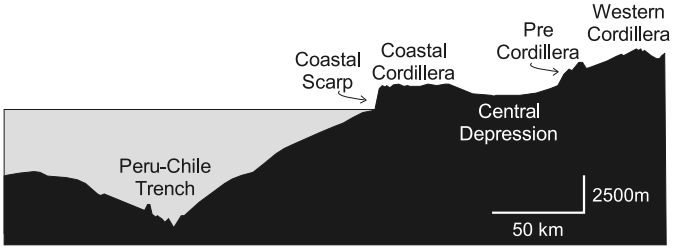

(b)

Fig. 1. (a) Main terrain units and structures of the study area. A–A′ shows line of section depicted in (b). Bold lines with triangles indicate thrusts; bold lines with solid rectangles indicate normal faults; half arrows indicate lateral movement along faults. Main type sections used in this study are located by (1) Caleta Buena; (2) El Magnifico and (3) Rocas Tortuga. (b) Topographic transect A–A′ showing the onshore to offshore topography of the study area and key terrain units.

affecting this important landscape element whilst a hyper-arid climate presents an environment which can conserve that evidence over suitably long timescales. With this in mind, we aim to document for the first time the regional scale of coastal giant landslides in the western Atacama Desert and explore their wider tectonic and climatic significance within this classic terrain setting.

2. Study area

The study area (Fig. 1) is located within the Central Andes which is often cited as the type example of a convergent continental margin, yet it is unusual in maintaining shear stresses across the subduction zone that are some three times higher (~37 MPa) than other convergent continental margins (Lamb, 2006). The stress build up is considered to be related to increased friction at the plate interface because of a lack of lubricating trench fill sediment (Von Huene and Ranero, 2003; Lamb and Davis, 2003). The relative lack of sediment offshore is related to the climatic aridity that has prevailed along this continental margin for much of the Neogene (e.g. Dunai et al., 2005). The response to the shear stress build up and lack of lubricating sediments has been to steepen the surface of the forearc wedge towards the trench through underplating beneath the Coastal Cordillera (Clift and Hartley, 2007). This has helped develop a relief of some 2 km

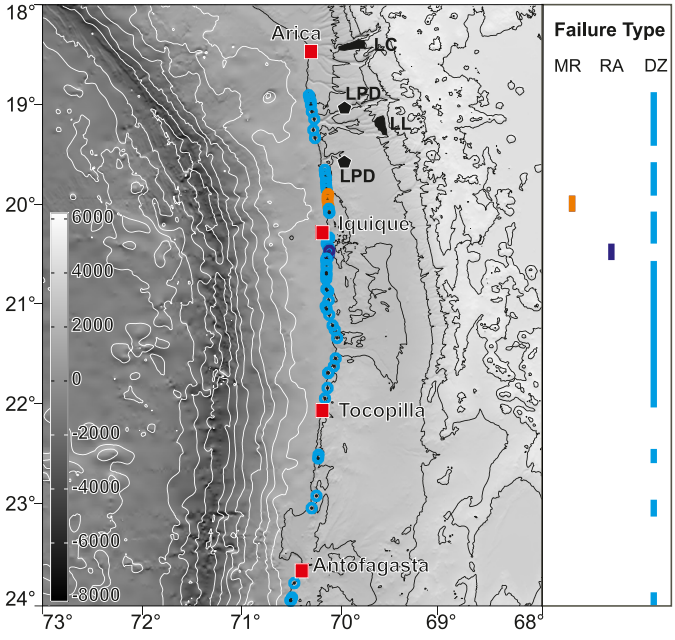

Fig. 2. Topography and landslide location in the Northern Chile study area. Bathymetry and elevation of the study area (source GEBCO 30′ Arc 2008 data). Contours are at 1 km intervals. Black circles indicate locations of giant coastal landsides (this study). Inland black areas represent the Lluta Collapse (LC) of Strasser and Schlunegger, 2005; Latagualla landslide (LL) of Pinto et al., 2008 and large-scale landslide prone drainages (LPD) identified by the authors but not discussed here. The preserved failure types are Multiple Rotational (MR); Rock Avalanche (RA) and Depletion Zone (DZ) as discussed in the text. These data are recorded in the supplementary information for this paper.

above sea level and an additional 7 km below sea level (Fig. 1) within a hyper-arid climate setting. Recent cosmogenic radionuclide (CRN) exposure dating using ^{21}Ne on quartz pebbles from alluvium in the Coastal Cordillera has highlighted negligible erosion rates over the last ~9 Ma (Dunai et al., 2005) suggesting, along with other data (e.g. nitrate and gypsum soils) that an arid/hyper-arid climate has prevailed across much of Northern Chile during this period (Hartley, 2003; Dunai et al., 2005; Evenstar et al., 2009) punctuated with low frequency, high magnitude rainstorm events, particularly in the south of the study area (e.g. Vargas et al., 2006; Placzek et al., 2010). The region is located within a seismically active terrain (Delouis et al., 1997; Spence et al., 1999) but historically is part of a well known seismic gap (Chlieh et al., 2004; Baker et al., 2013; Béjar-Pzarro et al., 2013; 450 km of coastline from 18°–23° south) with recurrence intervals in the order of 111 yr (Comte and Pardo, 1991). Recent research suggests that some 2000–9000 individual large plate boundary earthquakes have occurred in this region in the past 0.8 to 1 million yr (Baker et al., 2013). Although recent large earthquakes have been recorded close to the north and south of this gap (June 23rd 2001; southern Peru $Mw = 8.4$; July 30th 1995; Antofagasta $Mw = 8.1$, Chlieh et al., 2004) the last major event within the gap was in 1877. This generated a 25 m runup tsunami in Arica (Kulikov et al., 2005) and it is generally accepted that the region is now overdue its next megathrust event (Béjar-Pzarro et al., 2013).

Within the study area the Coastal Cordillera is up to 2.2 km high and 20 to 50 km wide (Fig. 1). It largely comprises basaltic andesites and granodiorites cut by N-S to NE-SW trending, landward-dipping, normal faults that bound a series of half-graben (Paskoff, 1978). The western margin of the Coastal Cordillera is represented by a coastal scarp – a prominent break in slope 600 to 1500 m high that runs for 700 km along the coastline of Northern Chile. Where the scarp is separated from the active coastal erosion by the narrow (<6 km wide) coastal plain it is considered

(a)

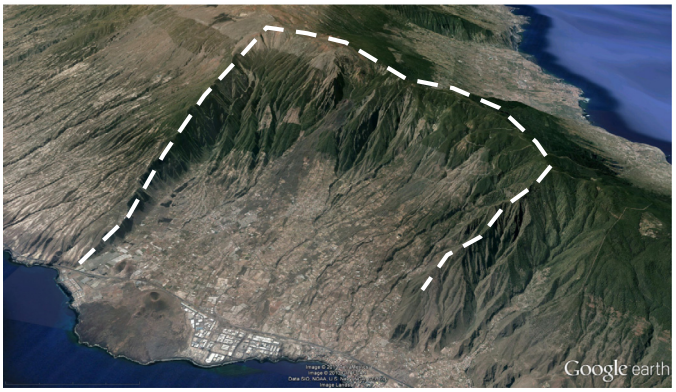

(b)

Fig. 3. Examples of giant landslides from the Canary Islands. (a) El Golfo, formed by a debris avalanche on the northwest flank of El Hierro is the best preserved and one of the youngest examples (13–17 ka; Masson et al., 2002). The depletion zone is all that can be seen above sea level. It is some 15 km across at its widest point with a 1000 m high scarp. Image courtesy of Google Earth (Image December 30th 2012). The depletion zone of Guimar, formed by a debris avalanche on the southeastern flank of Tenerife is older (?780–840 ka; Masson et al., 2002) and subaerially more poorly defined. The depletion zone is some 10 km across and the scarps are some 300–600 m in height. Image courtesy of Google Earth (Image March 18th 2012).

to represent a weathered palaeo-cliffline of mid-Miocene origin (Mortimer and Saric, 1972). Horse-shoe shaped scars 1 to 10 kms across are developed along the entire coastal scarp length (Fig. 2). These are morphologically consistent with the back scar of depletion zones reported from giant landslides in volcanic island terrains (Masson et al., 2002; Fig. 3); some of these depletion zones have associated subaerial accumulation zones but in most cases the displaced material has been deployed off-shore. In the latter, probably older, cases it is not possible to identify the individual accumulation zones off-shore from available imagery but it is possible to examine the off-shore components of older events within exposed Pliocene marine sedimentary sequences.

The absolute age of individual giant landslide scars is currently unknown. The presence of large event deposits (tsunami and landslide) are preserved within exposed Pliocene sediments that constitute the coastal plain (Hartley et al., 2001). Quaternary marine terraces preserve remnants of sea-level maxima from Oxygen Isotope Stages 5c, 5e, 7 and 9 (Ortlieb et al., 1996) that both pre- and post-date landslide features. These data suggest the preserved giant landslides span an age range from 0.1 ka–1 Ma and possibly up to the mid Miocene.

3. Coastal giant landslide characteristics

Using a combination of remote terrain analysis from an interpretation of aerial photographs and satellite imagery (Google Earth Professional) together with field geomorphological mapping, sedimentological, geological and structural data collection, more than 60 landslides have been located along the coastline of the study area (Fig. 2). This gives a mean occurrence of 1 landslide per 10 km of coastline which range in volume from 0.08 km^3 (El Magnifico, reported here) to 9 km^3 (Immediately north of Rocas Tortuga presented here). Although there is a lack of absolute dating evidence, the landslides can be grouped into two broad age categories based on their physical location in the landscape and relative degree of preservation: these are the more complete (accumulation and depletion zone preserved) and younger (mid-late Quaternary) failures and the less complete (depletion zone only preserved) and older (Plio/Pleistocene) failures (Table 1). Of these the latter are the most abundant, comprising some 90% of the preserved features (Fig. 2). Here we present type examples representative of the range of coastal landslides observed during this study (Table 1).

4. Mid-late quaternary landslides

The more complete (accumulation and depletion zone preserved) and younger landslides divide into two main types:

4.1. Multiple rotational

The type example of giant multiple rotational failures is located on a stretch of coastline north of Iquique at Caleta Buena where these features dominate the coastline (Figs. 1 and 4). At this point the coastal scarp forms part of the active coastline. The depletion zone is located in seaward dipping rocks comprising predominantly sedimentary strata overlying more massive Mesozoic basement material. The backscars are commonly delimited by predominantly NNW/SSE orientated vertical discontinuities (see linear backscar adjacent to the marked 'X' in Fig. 4(b)). The toe of the Caleta Buena landslide has been trimmed by marine erosion (Fig. 4(b)) so that the calculated volume (Table 1) is likely to be an underestimate of the actual volume displaced. The most recent failure at Caleta Buena (marked 2 on Fig. 4(b)) cuts older landslide features (marked 1 on Fig. 4(b)) suggesting sufficient time elapsed between different landslide events for the slope to stabilize.

4.2. Rock avalanche

The type example of a rock avalanche is El Magnifico and is taken from a stretch of coastline south of Iquique dominated by such failures (Figs. 1, 5 and 6). It has run out over Pleistocene marine terrace deposits which at this point cover the terrestrial coastal plain. The depletion zone comprises a mixed sedimentary, evaporitic and volcanic bedrock sequence. The accumulated landslide volume lies at the small end of giant landslides (Table 1) and represents a rock avalanche which would have been rapidly emplaced in 7 lobes (Fig. 5(b)). The morphology of the individual lobes and evidence from the quarry sections in the accumulation zone (Figs. 5(b) and 6(a)) are consistent with a 'sturzstrom' (Hsu, 1975). Within the depletion zone potential planes of failure are evident along bedding within the mixed sedimentary/volcanic succession (typically with a strike of 145 to 183° and a dip of 8 to 20° to the west). Joints and faults (Fig. 7) provide additional cross-cutting failure planes which describe the shape of the backscar (Fig. 5(b)).

5. Plio/Pleistocene landslide record

The relatively older part of the landslide record manifests itself as preserved on-shore depletion zones which occur across the entire study area but are best preserved northward of Tocopilla

Table 1
Giant landslide characteristics for the type localities described in the text.

Locality name	Caleta Buena	El Magnifico	Rocas Tortuga (depletion zone)	Costa Verde (accumulation zone)
Location	19°54′27.59″S 70° 7′7.02″W	20°27′41.14″S 70° 6′46.51″W	21°55′29.98″S 70° 8′18.91″W	20°27′9.35″S 70°9′36.67″W
Failure style	Multiple rotational	Avalanche	Rotational/avalanche	?avalanche
Backscar elevation (m)	943	873	1700	?
Depth of surface rupture (m)	200	119	300	?
Width of surface rupture (km)	3.3	0.93	3.4	?
Length of surface rupture (km)	2.2	1.4	3.1 (assuming 30° runout for initial failure)	?
Travel angle (°)	21	11.5	?5–10	?
*Volume (km^3)	0.8	0.08	1.67	?
†Volume with swelling/bulking factor (km^3)	NA	0.1	2.22	?
Accumulation zone	Subaerial (base of coastal scarp)	Subaerial (on coastal plain)	Off-shore (5–15 km) but not observed	Off-shore (~3 km) in coastal zone

Location information is based on location of the middle of the backscar based on the World Geodetic System (WGS) 84. For a more in depth descriptions of landslide terms used above see Griffiths (2005). *Volume calculated using half ellipsoid (WP/WLI, 1990). †Rock avalanche failure volume with swelling/bulking factor of 33% applied (after Nicoletti and Sorriso-Valvo, 1991).

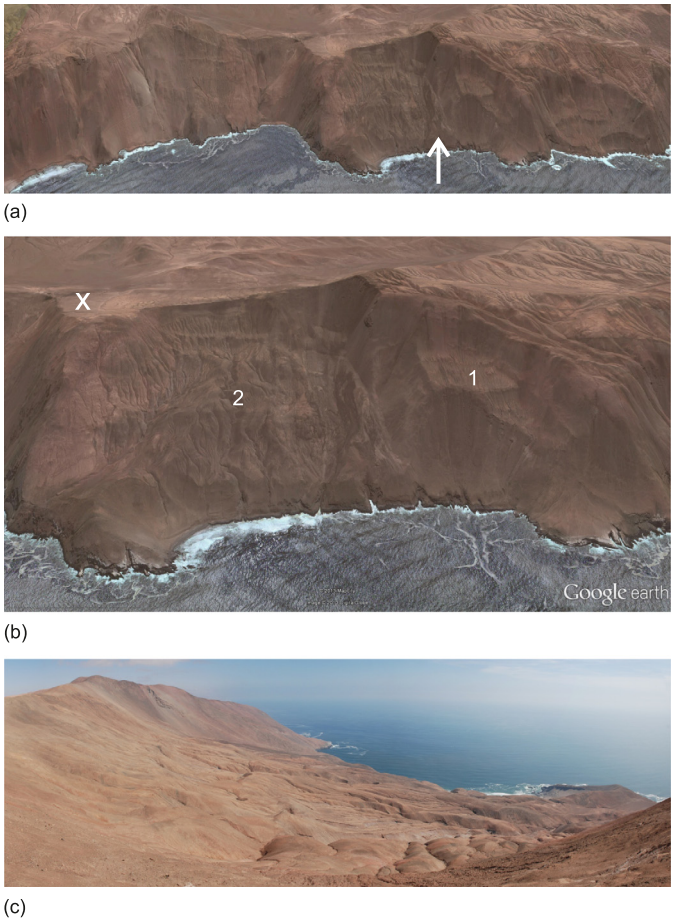

Fig. 4. Coastal Scarp dominated by Multiple rotational failures and type section (Caleta Buena). Here the coastal scarp forms part of the active coastline. (a) Oblique satellite image looking east over a 15 km length of coastline north of Iquique. White arrow indicates position of type locality. Image courtesy of the Google Earth Archive (Image May 19th 2006). (b) Oblique satellite image looking east over the type locality of Caleta Buena courtesy of the Google Earth Archive (Image January 4th 2011). '2' represents the main failure measured which is 3.3 km wide. Note this landslide has removed parts of an earlier landslide marked '1'. X marks where the field shot was taken in (c). Note cracking visible on imagery just to left of 'x'. (c) Field view taken looking south (right) from 'X' on (b). Field of view some 3 km across.

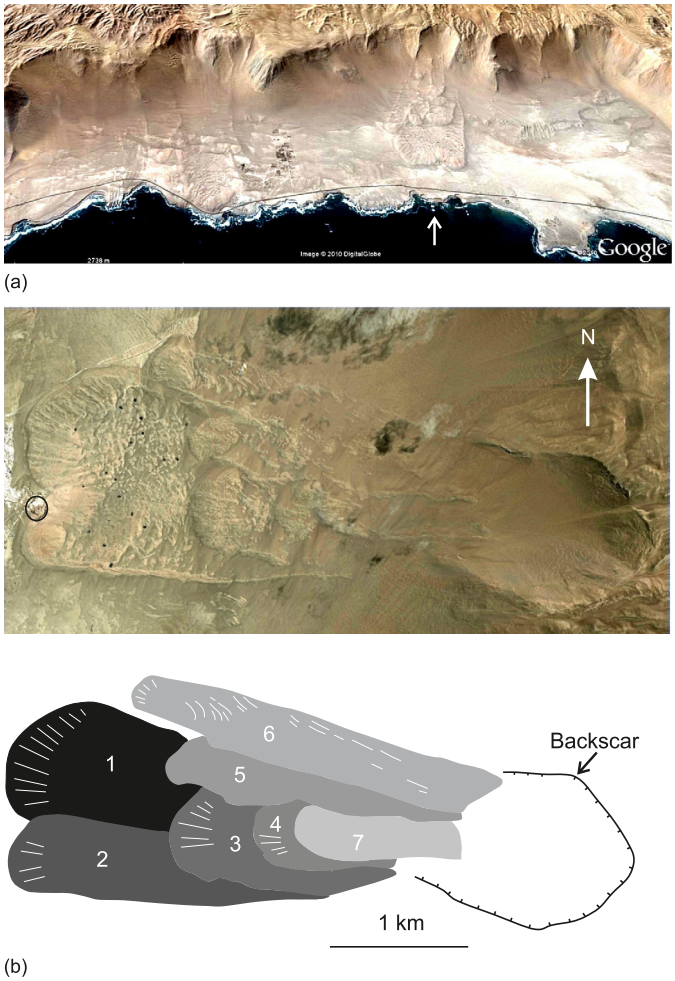

Fig. 5. Coastal scarp dominated by rock avalanches and type section El Magnifico. Here the coastal scarp is represented by a palaeo-cliff line. (a) Oblique satellite image courtesy of the Google Earth Archive (Image May 19th 2006) of 14 km of coastline south of Iquique showing rock avalanche failures. Type section is located above the white arrow. (b) Type locality El Magnifico. Satellite image courtesy of the Google Earth Archive (Image May 19th 2006). Simplified geomorphological map of the landslide system showing the 7 lobes (1 first to be emplaced, 7 last to be emplaced) drawn from remote and field mapping. Circled area at landslide toe locates the quarry section seen in Fig. 6(a).

(a)

(b)

Fig. 6. Field images of the El Magnifico type locality (a) quarry section through the toe of lobe 2 of the landslide. Note person for scale (circled) and irregular shear surface (arrowed) which marks the contact between lobes 1 and 2 (Fig. 4(b)). Location of quarry is indicated by circle in Fig. 4(b). (b) view up the landslide taken from the toe looking east towards the backscar located within the coastal scarp. Lateral boundaries and undulating ground forming the accumulation zone are clearly visible.

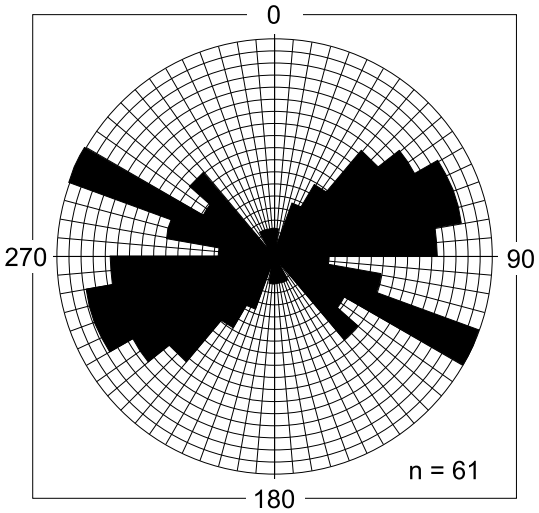

Fig. 7. Rose plot of joint and fracture orientations within the *in situ* local bedrock exposed at the locality of El Magnifico.

(Figs. 2, 8 and 9). The description of these as landslide depletion zones is based on their overall morphology (Fig. 8) which is comparable to those observed both in the better preserved part of the landslide record presented in this paper (e.g. Fig. 5) and those from other settings (e.g. Masson et al., 2002 and Fig. 3). The accumulation zone would have been deployed off-shore (Table 1) but marine erosion in this high energy coastal zone and lack of suitable near shore imagery does not allow the matching of individual accumulation zones with depletion zones. The off-shore accumulation zones, however, can be examined within the sedimentology of exhumed Pliocene shallow marine deposits (Fig. 9).

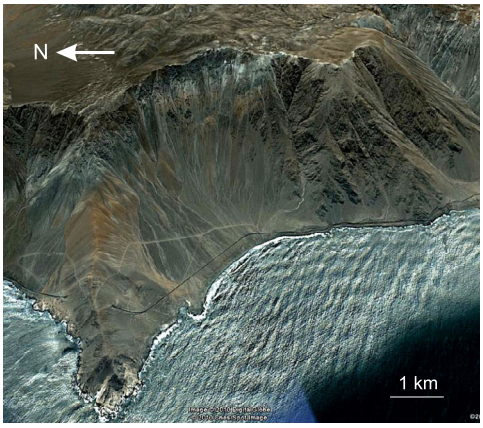

(a)

(b)

Fig. 8. Type example of relatively older (?Pliocene) landslide depletion zone: Rocas Tortuga. Accumulation zone will be located off-shore. (a) Satellite image oblique view courtesy of the Google Earth Image Archives (February 28th 2006); (b) Ground image looking south into the Rocas Tortuga depletion zone.

5.1. Depletion zone

The recognition of the more ancient failures is based on the occurrence of a series of horseshoe shaped scars along the coastal escarpment (Fig. 2). Rocas Tortuga (Fig. 8) is a typical example of such a feature. This depletion zone represents a complex but principally an initial multiple rotational landslide form (Soeters and Van Westen, 1996) which, as a first time failure, is likely to have had a travel angle (i.e. runout) of 30° or less (Table 1). Rocas Tortuga is developed in a dominantly volcanic bedrock succession and is cut into the active coastal cliff. The base of the depletion zone is cut by Quaternary marine surfaces which it therefore pre-dates. Rocas Tortuga forms a giant landslide of intermediate size along the coastal zone (Table 1). Given the scale of this landslide, following the initial failure secondary break-up movements are likely to resemble those associated with rock avalanches, comparable with the younger failures in the study area. Based on terrestrial sturzstrom studies (e.g. Hsu, 1975) and consistent with similar failures in the study area such as El Magnifico (Table 1) these type of failures can have travel angles in the order of 10°. In this case this would lead to the debris fan ending some 5 kms offshore. A 5° travel angle is more typical of the examples recorded from volcanic islands such as the Canary Islands (Masson et al., 2002), which start subaerially but enter water, and if this was the case at Rocas Tortuga then the debris fan would continue some 15 kms offshore.

5.2. Accumulation zone

Preserved within the Pliocene coastal plain sediments and truncated by Pleistocene marine terraces are the deposits of the off-shore component of large slope failures in beds up to 8 m

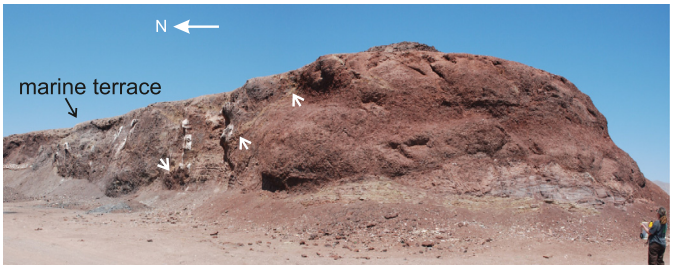

Fig. 9. Type example of relatively older (?Pliocene) landslide accumulation zone: Caleta Verde. Pliocene example of accumulation zone deposits preserved within a shallow marine sequence. Section is 6.5 m high. Note predominantly brecciated bedrock in upper section, and shear planes (arrowed) within the sequence. Basal contact is irregular with some large rip up blocks. Top of section is truncated by a marine terrace.

thick and in some cases extending laterally on kilometre-scales. Fig. 9 presents an example of what would have been an off-shore Pliocene landslide accumulation zone from the El Magnifico area. The top of this section is cut by a Pleistocene marine surface so the sequence is incomplete. The breccias are derived from local bedrock currently exposed in the shore platform and cliff section deposited within a shallow marine sedimentary sequence (Fig. 9). Thrust surfaces can be observed within the breccias which are consistent with those observed where lobe 2 contacts lobe 1 in the quarry section of El Magnifico (Fig. 6(a)). The base of the breccia in this example contains ripped up blocks of the local bedrock.

6. Discussion

The size of the giant landslides and their abundance along the coastline is controlled by 4 main factors: (1) topographic niche for their development provided by the coastal scarp, (2) preconditioning of the geology, (3) large subduction earthquakes to act as a final trigger and (4) hyperaridity which minimises fluvial erosion processes and preserves the landslide features over 10^3 to 10^6 yr timescales.

The available evidence suggests that the predominant style of landsliding was by a combination of rotational sliding and rock avalanche (sturzstrom). The morphology of El Magnifico (Fig. 5(b)) suggests that these latter events involved several pulses of lobe emplacement either in one or successive events possibly separated by a significant time gap. The preconditioning of the geology provides many deep seated potential failure surfaces in the form of sedimentary bedding, tectonic fault and joint planes (Fig. 7) and co-seismic cracking (Loveless et al., 2009).

Steepening of regional gradients by uplift is significant in pushing steeper elements of the landscape closer to catastrophic collapse but there also needs to be a suitable topographic niche to allow the movement. At the coast this is provided by the coastal scarp (reported here). Inland it is usually the incised valleys (e.g. Pinto et al., 2008). The large scale of the Coastal Cordillera slope failures, in a region dominated by a coastal scarp within a hyper arid climate and with no active volcanic edifices suggests that the final trigger for slope failure is large earthquake events (Wieczorek, 1996., Korup et al., 2007). Where the coastal scarp forms part of the active coastline (e.g. Caleta Buena, Figs. 1 and 2) marine undercutting cannot be ruled out as a possible trigger. On the Hawaiian Islands McMurtry et al. (2004) suggest that many of the giant landslides were triggered by eustatic rises in sea-level at the onset of interglacials during the Pleistocene. However events such as El Magnifico (Figs. 4 and 5) deposited subaerially above a marine surface and with no evidence for marine reworking clearly indicate it is not necessary to invoke marine interaction to explain the landslides on the coastal scarp.

Although there are no documented examples of giant landslides associated with historic large earthquakes in this region of Chile, this is not uncommon for events occurring prior to the mid 20th century across the globe (Keefer, 2002) due to a lack of records. However it is worthy of note that offshore surveys following the 27th February 2010 Maule earthquake (offshore central Chile, Mw 8.8) observed no large (>1 km^3) landslides. Völker et al. (2011) used these observations to suggest that frequent shaking may limit landslide volume by triggering more frequent but smaller landslide events. This may well limit the number of submarine off-shore giant landslides observed in Northern Chile. It should also be noted, however, that in coastal Northern Chile the bias in the earthquake record is towards low frequency, high magnitude megathrust earthquakes attributed to the high stress build up in the subduction zone thought to result from an absence of lubricating sediment in the trench (Lamb and Davis, 2003). Thus when the nature of this earthquake cycle is considered together with the lack of additional landslide trigger mechanisms (mainly moisture driven) as a result of the hyper-aridity, then the abundance of giant landslides in the on-shore geomorphic record may be explained. These factors combine to lessen the landslide frequency and allow the relief to grow to the point that higher magnitude, but less frequent events dominate the landslide record. The apparent abundance of landslides is further enhanced by their excellent preservation potential under such a climate.

The recognition of widespread coastal giant landslides in Northern Chile implies a significant, previously unreported hazard from this coastline in the form of both rapid catastrophic collapse and associated tsunami hazard affecting the major population centres of Southern Peru and Northern Chile. The multiphase emplacement of some of the events has significant ramifications for the propagation of any associated tsunami wave (as this type of failure tends to generate a larger number of lower amplitude waves than one single emplacement; Giachetti et al., 2011). Such events should not be underestimated and are capable of generating mega-tsunami (e.g. the earthquake triggered landslide events and associated tsunami recorded in Alaska in 1958 and 1964; Fritz et al., 2009; Suleimani et al., 2011).

Individual giant landslides associated with fold and fault structures and volcanic edifices have been documented previously from the western flank of the Andean Cordillera in Northern Chile. These include the western Precordillera (the Lluta Collapse 26 km^3, Strasser and Schlunegger, 2005; the Latagualla landslide 5.4 km^3 Pinto et al., 2008) and volcanic edifice collapse (the Socompa failure debris avalanche deposit of 26 km^3 and associated failures; e.g.. Wadge et al., 1995). Giant landslides have also been documented from the offshore region (Li and Clark, 1991, who identified a 91 km by 26 km block in the SeaMARC II survey off-shore Iquique, Fig. 1) whilst large-scale mass wasting of the slope has been observed in seismic, core and side-scan surveys for the off shore region in the study area (Li, 1995; Von Huene and Ranero, 2003; Vargas et al., 2005; Ranero et al., 2006 and Vargas et al., 2011). Although individual giant landslides have been previously documented and linked to regional tilting in the Precordillera region (e.g. Wörner et al., 2002) this is the first time that regionally extensive, giant terrestrial coastal landsliding has been identified in Northern Chile. These new data provide a previously unidentified and important geospatial continuum between the onshore and offshore landslide record, extending this record directly to the onshore area (Fig. 9). This implies that much of the slope from the top of the Coastal Cordillera to the trench – a vertical distance of 9 km – is close to failure. The coastal landslides tend to be more abundant (Fig. 2) but typically smaller than the giant landslides previously reported from the Precordillera. Although the Precordilleran landslides are infrequent, their presence does raise the possibility that in parts of Northern Chile (e.g. the Iquique area,

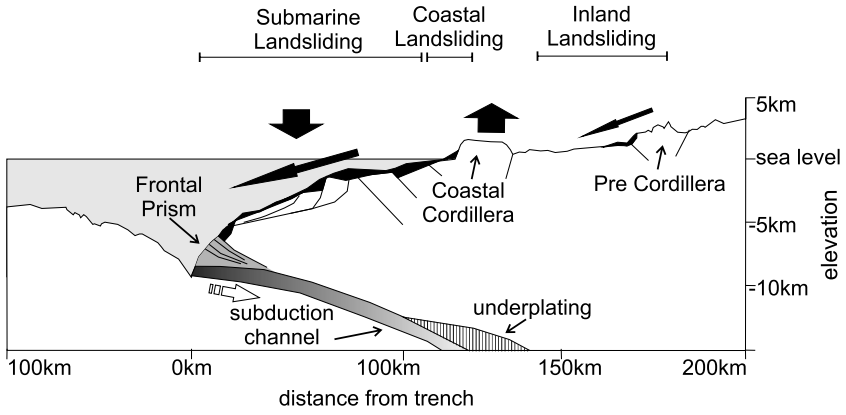

Fig. 10. Schematic model of the impact of underplating on the regional tectonic activity and geomorphology since the mid-Miocene. Adapted from Clift and Hartley (2007) and observations from multibeam bathymetric and off shore seismic data from Von Huene and Ranero, 2003. Areas of uplift and subsidence driven by underplating increasing the regional gradient are indicated by large vertical arrows. Thinner arrows indicate direction of mass movement events (giant landslides) transferring debris down regional gradient from the onshore to offshore area.

Fig. 2) the entire forearc wedge is close to critical and undergoing gravitational collapse over a vertical distance of 12 km during the Pliocene to Quaternary Periods.

The high stresses present across the Central Andean subduction zone are thought to be related to the absence of lubricating sediment in the trench (Lamb and Davis, 2003). This lack of sediment input is reflected in published off-shore sedimentation rates. In Northern Chile modern sedimentation rates were found to be low (0.04–0.17 $cm\,yr^{-1}$) compared to wetter areas of Southern Chile due to a decrease in on-shore precipitation and river runoff. Locally higher values recorded in off-shore Northern Chile were typically located in deeper water and areas of steeper continental shelf and are thought to reflect slumping processes (Muñoz et al., 2004). Thus through aridity and its impact on sedimentation rates and processes, climate controls the stress build up which is manifested in uplift of the Andean Cordillera. The climate also controls the geomorphic response of the forearc to uplift. In this hyper-arid regime the only effective geomorphic erosion mechanism for reducing relief is landsliding. Thus we would suggest that not only does climate allow the build up of the significant forearc topography in the Central Andes but it also controls the process by which the topography is reduced.

Steepening of the Central Andean forearc wedge in the late Neogene has been documented by Clift and Hartley (2007). They recognised that the position of the present day shoreline in Northern Chile has not moved significantly from the late Neogene, as beach and shoreface sediments of late Miocene, Pliocene and Pleistocene age are exposed in present day beach terraces. The forearc wedge taper must therefore have increased during this time period to accommodate the tectonic erosion rate of ~1–2 km/m.y. which has prevailed in this area over at least the last 20 m.y. (Von Huene and Ranero, 2003). We suggest that the terrestrial and submarine landslides could in part represent the geomorphic manifestation of late Neogene increased forearc taper in response to underplating (Fig. 10). It also is worthy of note that the younger and better preserved part of the landslide record can be found to the north of the study area around Iquique (Fig. 2) and the better preserved older record becomes more prolific north of Tocopilla to south of Iquique (Fig. 2). Whilst it is possible that some of the DZ sites in the inventory could be reinterpreted with more detailed analyses, even allowing for this the spatial distribution of landsliding is biased towards the coastline north of Tocopilla (Fig. 2). This area also corresponds spatially with the area identified by Mather and Hartley (2006) to have amplified Stream Gradient Index values which indicate elevated uplift rates (postulated to be in more than 1000 $mm\,y^{-1}$) for this stretch of coastline. It also corresponds with a general increase in aridity along the coastline (e.g. Placzek et al., 2010) which would serve to both maximise surface uplift (the balance between crustal uplift and erosion) and minimise their obscurity by other surface processes such as debris flows. The differential uplift along the coastline has been attributed to aseismic ridge subduction which may well account for spatial difference in uplift along the coastline (Hartley and Jolley, 1995; Mather and Hartley, 2006).

The hyper-arid climate that prevails along the western flank of the Central Andes has had a profound influence on orogenic uplift and erosion either directly, by influencing the nature of sediment transport and erosion, or indirectly by restricting sediment supply to the trench and lubrication of the subduction channel (e.g. Lamb and Davis, 2003). The possibility arises that changes in climate through time will have strongly influenced uplift and erosion rates in the Central Andes. If this is the case for the type example of a convergent continental margin, then it is likely that ancient examples will have been similarly influenced.

7. Conclusions

Giant landslides along coastal Northern Chile are both well preserved and prolific. Their presence is the geomorphic response to increased aridity and uplift which can be attributed on the largest scale to tectonic steepening along the Andean margin and at smaller (100 km) scales may reflect variations in uplift rates associated with aseismic ridge subduction along the plate margin. These factors during the Late Neogene have led to regional slope oversteepening. The trigger mechanism of such large events in a hyperarid, avolcanic setting is most likely large megathrust earthquakes, suggesting that the palaeolandslide record could contain yet unexplored valuable data on the recurrence of such events over Late Neogene timescales. Their presence implies a significant, previously unreported hazard from this coastline in the form of both rapid catastrophic collapse and associated tsunami hazard.

The coastal landslides in Northern Chile provide a continuum with submarine landslides present from close to the shoreline to over 7000 m water depth near the trench, indicating almost continuous slope failure over a vertical distance of 9 km. Slope failure may be in part attributed to increased forearc taper during the late Neogene as a result of underplating of material removed by tectonic erosion, and in part to differential uplift associated with more localised subduction characteristics. Forearc uplift and failure is strongly influenced by the hyper-arid climate of western South America through restricting: (1) sediment supply to the trench and thus promoting increased friction at the subduction

zone, (2) geomorphic erosion rates generating slope oversteepening, and (3) effective sediment transport processes to landsliding. The strong influence of climate on the development of the Central Andean convergent margin suggests that climate was also an important controlling factor in the development of convergent continental margins throughout Earth's history.

Acknowledgements

Mather and Hartley would like to acknowledge support from Royal Society Research Grant 24407.

Appendix A. Supplementary material

Supplementary material related to this article can be found online at http://dx.doi.org/10.1016/j.epsl.2013.10.019.

References

Baker, A., Allmendinger, R.W., Owen, L.A., Rech, J.A., 2013. Permanent deformation caused by subduction earthquakes in northern Chile. Nat. Geosci. 6, 492–496.
Béjar-Pzarro, M., Socquet, A., Armijo, R., Carrizo, D., Genrich, J., Simons, M., 2013. Andean structural control on interseismic coupling in the North Chile subduction zone. Nat. Geosci. 6, 462–467.
Chlieh, M., De Chablier, J.B., Ruegg, J.C., Armijo, R., Dmowska, R., Campos, J., Feigl, K.L., 2004. Crustal deformation and fault slip during the seismic cycle in the North Chile subduction zone, from GPS and InSAR observations. Geophys. J. Int. 158, 695–711.
Clague, D.A., Moore, J.G., 2002. The proximal part of the giant submarine Wailau landslide, Molokai, Hawaii. J. Volcanol. Geotherm. Res. 113, 259–287.
Clift, P.D., Hartley, A.J., 2007. Slow rates of subduction erosion and coastal underplating along the Andean margin of Chile and Peru. Geology 35, 503–506.
Comte, D., Pardo, M., 1991. Reappraisal of great historical earthquakes in the northern Chile and southern Peru seismic gaps. Natural Hazards 4, 23–44.
Delouis, B., Monfret, T., Dorbath, L., Pardo, M., Rivera, L., Comte, D., Haessler, H., Caminade, J.P., Ponce, L., Kausel, E., Cisternas, A., 1997. The M-w = 8.0 Antofagasta (northern Chile) Earthquake of 30 July 1995: A precursor to the end of the large 1877 gap. Bull. Seismol. Soc. Am. 87, 427–445.
Dunai, T.J., Lopez, G.A.G., Juez-Larre, J., 2005. Oligocene–Miocene age of aridity in the Atacama Desert revealed by exposure dating of erosion-sensitive landforms. Geology 33, 321–324.
Evenstar, L., Hartley, A.J., Stuart, F.M., Mather, A.E., Rice, C., Chong, G., 2009. Multiphase development of the Atacama Pediplain recorded by cosmogenic ^{3}He exposure ages: implications for Cenozoic climate change in western South America. Geology 37, 27–30.
Fritz, H.M., Mohammed, F., Yoo, J., 2009. Lituya Bay Landslide impact generated mega-tsunami 50th anniversary. Pure Appl. Geophys. 166, 153–175.
Giachetti, T., Paris, R., Kelfoun, K., Pérez-Torrado, F.J., 2011. Numerical modelling of the tsunami triggered by the Güìmar debris avalanche, Tenerife (Canary Islands): comparison with field-based data. Mar. Geol. 284, 189–202.
Griffiths, J.S., 2005. Landslides. In: Fookes, P.G., Lee, E.M., Gilligan, G. (Eds.), Geomorphology for Engineers. Whittles, pp. 173–217.
Hartley, A.J., 2003. Andean uplift and climate change. J. Geol. Soc. Lond. 160, 7–10.
Hartley, A.J., Jolley, E.J., 1995. Tectonic implications of Late Cenozoic sedimentation from the Coastal Cordillera of Northern Chile (22–24 degrees). J. Geol. Soc. 152, 51–63.
Hartley, A., Howell, J., Mather, A.E., Chong, G., 2001. A possible Plio-Pleistocene tsunami deposit Hornitos, northern Chile. Rev. Geol. Chile 28, 117–125.
Hsu, K.J., 1975. Catastrophic debris streams (sturzstroms) generated by rockfalls. Bull. Geol. Soc. Am. 86, 129–140.
Keating, B.H., Mcguire, W.J., 2000. Island edifice failures and associated tsunami hazards. Pure Appl. Geophys. 157, 899–955.
Keefer, D.K., 2002. Investigating landslides caused by earthquakes—A historical review. Surv. Geophys. 23, 473–510.
Korup, O., Clague, J.J., Hermanns, R.L., Hewitt, K., Strom, A.L., Weidinger, J.T., 2007. Giant landslides, topography, and erosion. Earth Planet. Sci. Lett. 261, 578–589.
Kulikov, E.A., Rabinovich, A.B., Thomson, R.E., 2005. Estimation of tsunami risk for the coasts of Peru and northern Chile. Natural Hazards 35, 185–209.
Lamb, S.H., 2006. Shear stresses on megathrusts: Implications for mountain building behind subduction zones. J. Geophys. Res., Solid Earth 111. Article Number: B07401.
Lamb, S., Davis, P., 2003. Cenozoic climate change as a possible cause for the rise of the Andes. Nature 425, 792–797.
Loveless, J.P., Allmendinger, R.W., Pritchard, M.E., Garroway, J.L., Gonzalez, G., 2009. Surface cracks record long-term seismic segmentation of the Andean margin. Geology 37, 23–26.
Li, C., 1995. Forearc structures and tectonics in the southern Peru—northern Chile Continental Margin. Mar. Geophys. Res. 17, 97–113.
Li, C., Clark, A.L., 1991. SeaMARC II study of a giant submarine slump on the northern Chile continental slope. Mar. Geotechnol. 10, 257–268.
Masson, D.G., Watts, A.B., Gee, M.J.R., Urgeles, R., Mitchell, N.C., Le Bas, T.P., Canals, M., 2002. Slope failures on the flanks of the western Canary Islands. Earth-Sci. Rev. 57, 1–35.
Mather, A.E., Hartley, A.J., 2006. The application of drainage system analysis in constraining spatial patterns of uplift in the Coastal Cordillera of northern Chile. In: Willett, S.D., Hovius, N., Brandon, M.T., Fisher, D.M. (Eds.), Tectonics Climate and Landscape Evolution. In: Geological Society of America Special Papers, vol. 398, pp. 87–99.
McMurtry, G.M., Watts, P., Fryer, G.J., Smith, J.R., Imamura, F., 2004. Giant landslides, mega-tsunamis, and paleo-sea level in the Hawaiian Islands. Mar. Geol. 203, 219–233.
Moore, J.G., Bryan, W.B., Luswig, K.R., 1994. Chaotic deposition by a giant wave, Molokai, Hawaii. Geol. Soc. Am. Bull. 106, 962–967.
Mortimer, C., Saric, N., 1972. Landform evolution in the coastal region of Tarapacà Province Chile. Rev. Géomorph. Dyn. 21, 162–170.
Muñoz, P., Lange, C.B., Gutiérrez, Hebbeln D, D., Salamanca, M.A., Dezileau, L., Reyss, J.L., Benninger, L.K., 2004. Recent sedimentation and mass accumulation rates based on $_{210}$Pb along the Peru–Chile continental margin. Deep-Sea Res. II 51, 2523–2541.
Nicoletti, P.G., Sorriso-Valvo, M., 1991. Geomorphic controls of the shape and mobility of rock avalanches. Geol. Soc. Am. Bull. 103, 1365–1373.
Ortlieb, L., Zazo, C., Goy, J.L., Hillaire-Marcel, C., Ghaleb, B., Cournoyer, L., 1996. Coastal deformation and sea-level changes in the northern Chile subduction area (23 degrees S) during the last 330 ky. Quat. Sci. Rev. 15, 819–831.
Placzek, C.J., Matmon, A., Granger, D.E., Quade, J., Niedermann, S., 2010. Evidence for active landscape evolution in the hyperarid Atacama from multiple terrestrial cosmogenic nuclides. Earth Planet. Sci. Lett. 295, 12–20.
Paskoff, R., 1978. Sur l'évolution geomorphologique du grand escarpement côtier du désert Chilien. Geog. Phys. Quat. 32, 351–360.
Pinto, L., Herail, G., Sepulveda, S.A., Krop, P., 2008. A Neogene giant landslide in Tarapaca, northern Chile: A signal of instability of the westernmost Altiplano and palaeoseismicity effects. Geomorphology 102, 532–541.
Ranero, C.R., Von Huene, R., Weinrebe, W., Reichert, C., 2006. Tectonic processes along the Chile Convergent Margin. In: Oncken, O., Chong, G., Franz, G., Giese, P., Götze, H., Ramos, V., Strecker, M.R., Wigger, P. (Eds.), The Andes: Active Subduction Orogeny. Springer, pp. 91–121.
Soeters, R., Van Westen, C.J., 1996. Slope instability. Recognition, analysis and zonation. In: Turner, A.K., Schuster, R.L. (Eds.), Landslide: Investigations and Mitigation. Special Report 247. Transportation Research Board, National Research Council, National Academy Press, Washington, DC, pp. 129–177.
Spence, W., Mendoza, C., Engdahl, E.R., Choy, G.L., Norabuena, E., 1999. Seismic subduction of the Nazca Ridge as shown by the 1996–97 Peru earthquakes. Pure Appl. Geophys. 154, 753–776.
Strasser, M., Schlunegger, F., 2005. Erosional processes. Topographic length scales and geomorphic evolution in arid climatic environments: the Lluta collapse, northern Chile. Int. J. Earth Sci. 94, 433–446.
Suleimani, E., Nicolsky, D.J., Haeussler, P.J., Hansen, R., 2011. Combined effects of tectonic and landslide-generated tsunami Runup at Seward, Alaska during the M (W) 9.2 1964 earthquake. Pure Appl. Geophys. 168, 1053–1074.
Vargas, G., Ortlieb, L., Chapron, E., Valdes, J., Marquardt, C., 2005. Paleoseismic inferences from a high-resolution marine sedimentary record in northern Chile (23-8S). Tectonophysics 399, 381–398.
Vargas, G., Rutllant, J., Ortlieb, L., 2006. ENSO tropical–extratropical climate teleconnections and mechanisms for Holocene debris flows along the hyperarid coast of western South America (17°–24°S). Earth Planet. Sci. Lett. 249, 467–483.
Vargas, G., Palacios, C., Reich, M., Luo, S., Shen, C., González, G., Wu, Y., 2011. U-series dating of co-seismic gypsum and submarine paleoseismology of active faults in Northern Chile (23°S). Tectonophysics 497, 34–44.
Völker, D., Scholz, F., Geersen, J., 2011. Analysis of submarine landsliding in the rupture area of the 27 February 2010 Maule earthquake, Central Chile. Mar. Geol. 288, 79–89.
Von Huene, R., Ranero, C.R., 2003. Subduction erosion and basal friction along the sediment-starved convergent margin off Antofagasta Chile. J. Geophys. Res., Solid Earth 108 (B2), 2079.
Wadge, G., Francis, P.W., Ramirez, C.F., 1995. The Socompa collapse and avalanche event. J. Volcanol. Geotherm. Res. 66, 309–336.
Ward, S.N., 2001. Landslide tsunami. J. Geophys. Res., Solid Earth 106, 11201–11215.
Whelan, F., Kelletat, D., 2003. Submarine slides on volcanic islands – a source for mega-tsunamis in the Quaternary. Progr. Phys. Geogr. 27, 198–216.
Wieczorek, G.F., 1996. Landslide triggering mechanisms. In: Turner, A.K., Schuster, R.L. (Eds.), Landslides: Investigation and Mitigation. Special Report 247. Transportation Research Board, National Academy Press, Washington DC, pp. 76–90.
Wörner, G., Uhlig, D., Kohler, I., Seyfried, H., 2002. Evolution of the West Andrean Escarpment at 18°S (N. Chile) during the last 25 Ma: uplift, erosion and collapse through time. Tectonophysics 345, 183–198.
WP/WLI, 1990. Suggested method for reporting a landslide. Bull. Int. Assoc. Eng. Geol. 41, 5–12.